Effect of Preparation Conditions on the Adsorption of Heavy Metal Ions from Aqueous Solution by Mesoporous Silica Materials Prepared Using Organic Template (HDTMAB)

Ling-Chu Lin, Munusamy Thirumavalavan, Ying-Ting Wang, and Jiunn-Fwu Lee*

Graduate Institute of Environmental Engineering, National Central University, Chung-Li, Taoyuan County, 320, Taiwan

This paper describes the simple hydrothermal preparation of self-adsorbing mesoporous materials using hexadecyltrimethyl ammoniumbromide (HDTMAB) as the template without any functionalization. The template was readily removed upon calcination, as confirmed through Fourier transform infrared spectroscopic analysis. The effects of preparation methods were explored under various experimental conditions. We found that the temperature, time, calcination conditions, and pH all affected the distribution of pore sizes and the surface area, whereas higher pH (strong base) did not favor the preparation of a porous medium because of OH inhibition. We obtained a relatively high surface area (1568.72 $m^2 \cdot g^{-1}$) and large pore size (3.07 nm) under the optimal reaction conditions. A study of the Langmuir adsorption of metal ions (e.g., Pb^{2+}, Cu^{2+}, Ni^{2+}) revealed that it was a physical phenomenon with the maximum adsorption occurring for the sample prepared under the optimized experimental conditions, with Pb^{2+} (6.61 $mg \cdot g^{-1}$) exhibiting enhanced adsorption relative to Cu^{2+} (3.46 $mg \cdot g^{-1}$) and Ni^{2+} (2.25 $mg \cdot g^{-1}$) because of its larger ionic radius and higher electronegativity. Thus, such as-synthesized mesoporous materials hold great potential for use in the removal of heavy metal ions from aqueous solutions compared to commercially available powdered activated carbon (PAC).

Introduction

Although the removal of pollutants from wastewaters[1,2] can be performed using various technologies such as precipitation, ion exchange, membrane filtration, and reverse osmosis, these methods can have several disadvantageous features such as expensive equipment, continuous replenishment of chemicals, and failure to meet the Environmental Protection Agency requirements.[3,4] Considering the limitations of conventional methods for metal removal, the most promising alternative method appears to be the adsorption process. In addition, adsorption is superior to other techniques for water reuse in terms of the initial cost, simplicity of design, ease of operation, and insensitivity to toxic substances.[5,6] The development of improved adsorbents for the removal of toxic heavy metal ions from wastewater remains a continuing research objective for environmental pollution control processes. Mesoporous materials have great potential for use in environmental processes, and considerable effort has been devoted to the preparation of mesoporous adsorbents because of their unique large surface areas, well-defined pore sizes, and controllable surface properties.[7−9] In such preparations, surfactant molecules are generally used to form supramolecular assemblies in solution, either through electrostatic surfactant−precursor assembly interactions or hydrogen bonding. Subsequent surfactant removal results in a solid ordered material possessing high porosity which makes these materials very attractive for applications[10] such as catalytic supports, sensors, and adsorbents. The use of mesoporous silicas as heavy metal ion adsorbents has been widely studied recently.[11−16] Although such adsorbents generally require specific binding sites for heavy metal ions, most mesoporous materials do not possess such surface properties. Accordingly, an efficient approach[17−20] has been developed in which functional monolayers are chemically bonded to the surfaces of supports. In general, the surfaces of most of the mesoporous materials can be chemically modified to enhance their surface properties. With the increasing demand for economical large-scale water treatment applications, the development of novel, low-cost, stable, and efficient sorbents remains a great and significant challenge. In this paper, we report the hydrothermal synthesis of stable self-adsorbing (as-synthesized) porous adsorbents possessing improved surface characteristics for use in environmental remediation of various metal ions without any preceding functionalization (surface modification). The mesoporous materials should exhibit excellent structural flexibility and thermal and mechanical stability, which should be alterable by varying the synthetic conditions. Optimizing the synthetic conditions is the greatest challenge when searching for novel mesoporous adsorbents, and hence the synthesis, characterization, and use of mesoporous materials are all of considerable fascination to researchers. In this study, we attempted to integrate our recent efforts to synthesize mesoporous materials that function as adsorbents for metal ions such as Cu^{2+}, Ni^{2+}, and Pb^{2+}. We synthesized ordered mesoporous materials using surfactant micellar structures as templates that were subsequently removed through thermal treatment. We sought to clarify the effects of the preparation methods on the properties of the self-adsorbing mesoporous materials and to illustrate their application as adsorbents. We found that the hydrothermal synthesis was readily controlled by varying the temperature, time, filtration, and pH. Comparison with the adsorption behavior of analogous mesoporous materials confirmed that the reported mesoporous materials in this study possess several advantageous properties

* Corresponding author. E-mail: jflee@ncuen.ncu.edu.tw. Phone: +886-3-4227151-34658. Fax: +886-3-4226742.

10.1021/je1002253
Published on Web 07/19/2010

Table 1. Mesoporous Materials Prepared under Various Experimental Conditions

sample	pH	time (h)	temp (°C)	calcination temp (°C)	filtration (exhaust or dialysis membrane)	drying (oven or feeze)
ZC-16	10	24	100	600	exhaust	oven
ZC-16-12H	10	12	100	600	exhaust	oven
ZC-16-48H	10	48	100	600	exhaust	oven
ZC-16-96H	10	96	100	600	exhaust	oven
ZC-16-168H	10	168	100	600	exhaust	oven
ZC-16-60	10	24	60	600	exhaust	oven
ZC-16-80	10	24	80	600	exhaust	oven
ZC-16-500	10	24	100	500	exhaust	oven
ZC-16-700	10	24	100	700	exhaust	oven
ZC-16-C	10	24	100	600	dialysis memb.	freeze
ZC-16-P9	9	24	100	600	exhaust	oven

relative to that of commercially available powdered activated carbon (PAC).

Experimental Section

Chemicals. Standard metal ion solutions were obtained commercially. All the chemicals and reagents used in this study were of Analar grade (AR grade) and used as supplied without further purification.

Preparation of Mesoporous Materials (ZC-16) Using HDTMAB. An aqueous solution of hexadecyltrimethyl ammoniumbromide (HDTMAB) was shaken at 40 °C for 30 min at 150 rpm in a Lab-line orbit environ shaker. Sodium silicate solution (35 % 0.05 M, pH = ca. 11 or 12) comprising 16.22 $g \cdot mol^{-1}$ of SiO_2 (assay 27 %) and 4.96 $g \cdot mol^{-1}$ of Na_2O (assay 8 %) was prepared by shaking aqueous sodium silicate solution at 150 rpm for 30 min at 40 °C. The HDTMAB solution was added slowly to the sodium silicate solution over a period of 1 h under stirring, and after complete addition, the reaction mixture was diluted using an appropriate amount of deionized water. Next, 1 M H_2SO_4 was added to maintain the pH at ca. 10. The reaction mixture was heated at 100 °C for 24 h. After cooling, the sample was washed several times with deionized water, filtered, and dried at 100 °C in an oven for 12 h. The final sample (herein referred to as ZC-16) was obtained after calcination at 600 °C. ZC-16 was prepared and referred to under different experimental conditions as shown in Table 1.

Batch Adsorption Studies. The adsorption of Cu^{2+}, Ni^{2+}, and Pb^{2+} was investigated in batch equilibrium experiments. Stock solutions of metal ions (1.0 $g \cdot L^{-1}$) were prepared using the obtained standard solutions in distilled water. The temperature was maintained at 28 °C. The experiments were performed at pH 3 in 250 mL conical flasks containing metal ion solutions [(1 to 8) $mg \cdot L^{-1}$] and the adsorbents (0.1 g) and shaken for 24 h at 150 rpm in a Lab-line orbit environ shaker.

Analytical Procedure. The adsorption of metal ions from aqueous solutions was studied. After the desired incubation period for each batch, the aqueous phases were separated from the materials, and the concentration of metal ions was measured using a Varian AA-400 atomic absorption spectrophotometer (AAS).

The amount of metal adsorbed was calculated using the following equation

$$q_e = [(C_0 - C)V]/M$$

where q_e is the amount of metal ion adsorbed per unit amount of the adsorbent ($mg \cdot g^{-1}$); C_0 and C are the concentrations of the metal ion in the initial solution ($mg \cdot L^{-1}$) and after adsorption, respectively; V is the volume of the adsorption medium (L); and M is the amount of the adsorbent (g). The value of q_{max} was calculated from q_e using Langmuir linear isotherms, and the corresponding values were obtained using a linear method.

Desorption and Reuse of the Adsorbents. The reusability of the adsorbents for metal ion adsorption was determined. Measurements were repeated after 4 to 5 consecutive adsorption−desorption cycles using the same adsorbent, and the maximum deviation was found to be ± 4 %. The desorption of metal ions was measured in a 10 mM $HCl:HNO_3$ solution. The adsorbents with metal ions were placed in the desorption medium and stirred at 150 rpm for 60 min at 25 °C. The final metal ion concentration in the aqueous phase was determined by using an Atomic Absorption Spectrophotometer (AAS), as described above. The desorption ratio was calculated from the amount of metal ion adsorbed by the adsorbents and the final metal ion concentration in the desorption medium using the following equation

Desorption ratio (%) =
amount of metal ions desorbed to the elution medium)·
100/(amount of metal ions adsorbed onto adsorbents)

Characterization Techniques. The average pore diameter and specific surface area [Brunauer−Emmett−Teller (BET) surface and pore volume] were measured using a Quantochrome NOVA 1000. The adsorbents were analyzed using X-ray diffraction (XRD) and scanning electron microscopy (SEM). XRD patterns were obtained at room temperature using a Mac Science M3X model 1030 instrument equipped with a Cu Kα X-ray source (40 kV and 20 mA). SEM was performed using an HITACHI-S-800 field emission scanning electron microscope. The surface composition was calculated through elemental analysis using energy dispersive spectroscopy (EDS) combined with SEM. Fourier transform infrared (FT-IR) spectra were recorded using a Neclit 6700 model spectrometer. A LM-595R rotary incubator (YIH DER Company) was used in the experiments requiring incubation. The pH was determined using a Jenco 6171 microcomputer-based bench pH meter.

Results and Discussion

To study the effects of the preparation methods, we varied several experimental parameters such as hydrothermal temperature, time, pH, calcination conditions, filtration, and drying as shown in Table 1. The techniques FT-IR spectroscopy, BET, SEM, and XRD were used to characterize the resulting as-synthesized mesoporous materials. We obtained various mesoporous materials with different surface areas and pore sizes under the various experimental conditions (see Table S1, Supporting Information). In addition, in this study we also compared the activities of these mesoporous materials as well as their adsorption behavior toward various metal ions.

FT-IR Spectroscopy, BET, SEM, TEM, and XRD. The surface compositions of the mesoporous materials were calcu-

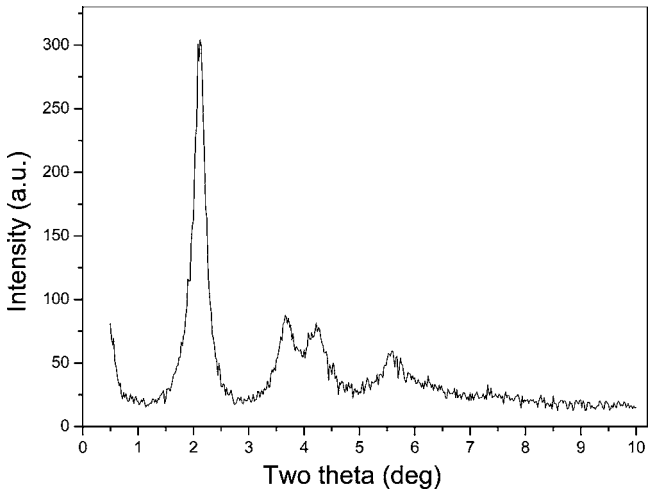

Figure 1. XRD patterns of ZC-16.

lated using EDS elemental analysis. The Si:C ratio for ZC-16 was 0.96 (Si = 49.20 %; C = 50.80 %) confirming that the surfactant remained throughout the synthesis.[21] The experimental data show that varying the synthetic conditions affected the specific surface area and pore size distribution. Thus, we compared the changes in surface areas and pore sizes of the mesoporous materials synthesized under various preparation conditions. Figure 1 shows the XRD patterns of ZC-16 which exhibits peaks (2θ) at 2.20° (d_{100} = 4.03 nm), 3.90° (d_{110} = 2.26 nm), 4.20° (d_{200} = 2.10 nm), and 5.60° (d_{210} = 1.58 nm). These peaks are indicative of typical silicate mesoporus materials (MCM-41), and it is identified as the thermally stable porous medium having a hexagonal lattice structure with a unidimensional pore distribution.[21,22] The mesoporous materials synthesized under various experimental conditions were characterized using FT-IR spectroscopy to confirm the nature of the functional groups before and after removing the organic template. The peaks at 800 cm^{-1} and 1082 cm^{-1} are due to symmetric and asymmetric ν(Si−O−Si); the peak at 963 cm^{-1} is due to terminal ν(Si−OH); the peak at 2800 cm^{-1} is due to $\nu(CH_3)$; the peak at 2920 cm^{-1} is due to $\nu(CH_2)$; and the peak at 3480 cm^{-1} is due to ν(OH) and hydrogen-bonded ν(Si−OH). The disappearance of the sharp peaks at 2800 cm^{-1} and 2920 cm^{-1} in the spectra of (see Figure S1, Supporting Information) the meosoporus materials after removing HDTMAB confirms the complete removal of this template. The SEM morphological studies of the mesoporous materials confirm the presence of uniformly distributed well-defined holes on the surface. The detailed study of the SEM reports that the different experimental conditions affected the structure and pore dimensions[21] of the mesoporous materials as shown in Figure 2.

N_2 Adsorption Isotherms. The obtained nitrogen adsorption isotherms (see Figure S2, Supporting Information) obviously convey that all the samples exhibited the same adsorption behavior, and the isotherms were type IV curves[23] in which the hysteresis was not obvious initially (it may occur only in the high relative pressure range). At low relative pressure (P/P_0 = 0:3) the adsorbed volume increased linearly upon increasing the pressure. This region corresponds to a monolayer−multilayer adsorption on the pore walls. Increasing the value of P/P_0 from 0.3 and 0.4, we observed a sharp increase

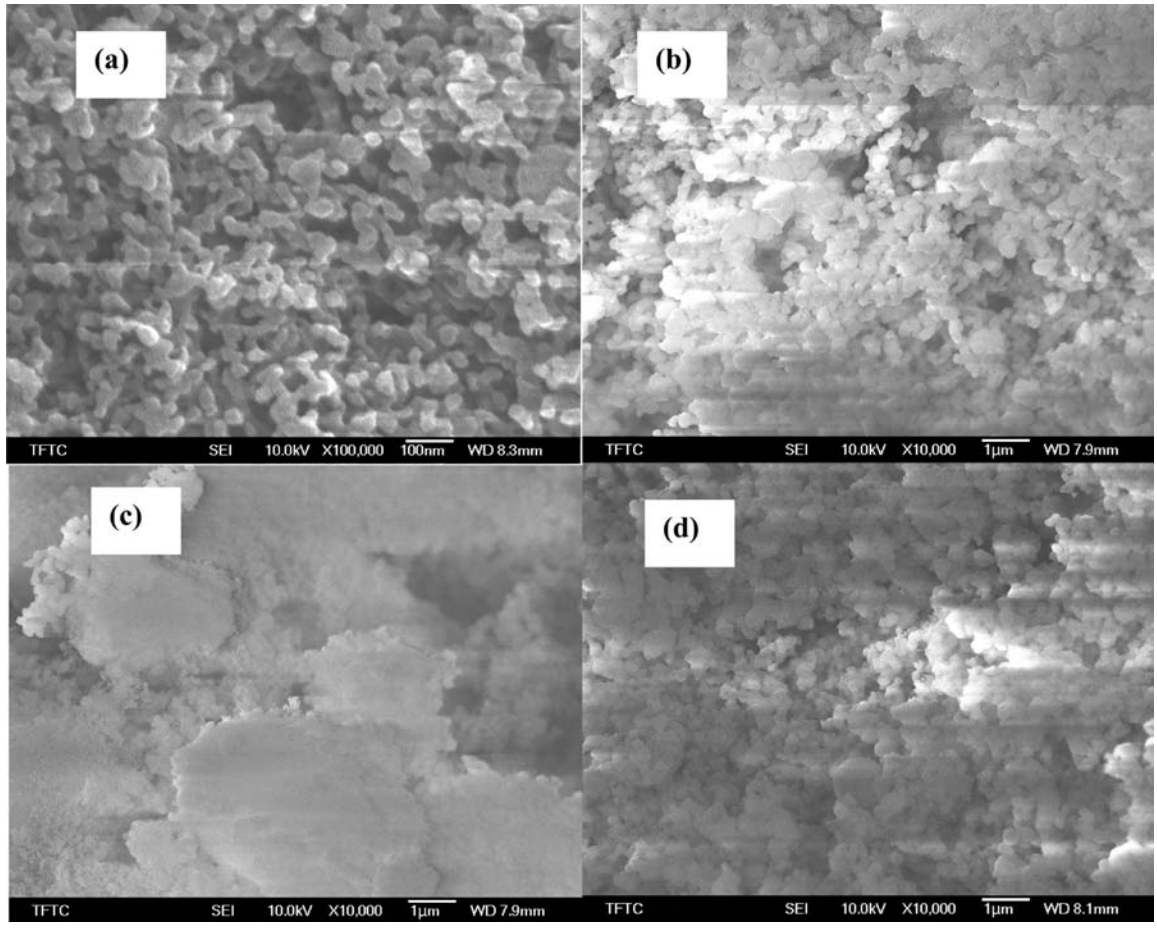

Figure 2. SEM images of (a) ZC-16, (b) ZC-16-12H, (c) ZC-16-C, and (d) ZC-16-P9.

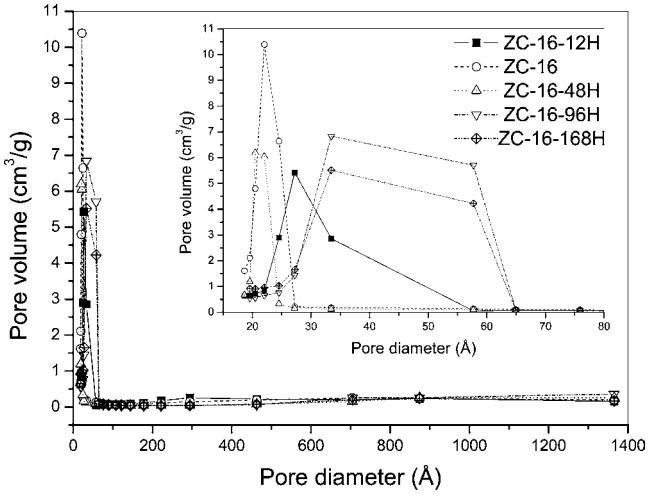

Figure 3. Effect of hydrothermal time on BJH pore distribution.

in the adsorbed volume, which we attribute to capillary condensation. At higher relative pressures, multilayer adsorption occurred on the external surface, resulting in a gradual increase in the adsorbed volume. At a value of P/P_0 of 1, saturation was reached indicating that all of the mesopores were filled with the condensed adsorbents. The isotherm for the mesoporous materials exhibits a sharp inflection characteristic of capillary condensation within a narrow pore size distribution, where the value of P/P_0 of the inflection point is related to the average diameter of the pores.[24] These N_2 adsorption data confirmed the uniformity of the pore size distribution of the samples.

Effect of Heating Time. To investigate the effect of different heating times, the hydrothermal synthesis was carried out under different heating times at 100 °C. The mesoporous materials obtained after 24 h (ZC-16) had the largest surface area among all the related samples (see Table S1, Supporting Information). The lowest surface area existed for the medium obtained after 7 days (ZC-16-168H). This result suggests that a longer heating time results in drying of the water content of the medium and hence a significant decrease in the surface area of the porous medium. In contrast, we did not observe any significant changes (only small random variations) in the average pore sizes of the media upon varying the hydrothermal heating times. The plot of pore volume with respect to pore size is shown in Figure 3, which reveals the effective pore size engineering. The pore size distribution was accumulated (narrow) and random over a wide range,[21] and the observed BJH distributions for ZC-16-96H and ZC-16-168H were large. Mesopores having a broad distribution of pore diameters around (20 to 70) Å were present. A longer hydrothermal heating process led to an increase in the pore size distribution, but it decreased the surface area of the porous medium significantly.

Effect of Hydrothermal Temperature. The different porous media ZC-16-60, ZC-16-80, and ZC-16 were obtained at various hydrothermal temperatures of 60 °C, 80 °C, and 100 °C, respectively. From the experimental results, we found that increasing the hydrothermal temperature favored the formation of porous materials having large surface areas. We observed a general increase in the surface area after increasing the synthesis temperature from (60 to 100) °C (see Table S1, Supporting Information). This increase in temperature corresponds to an increase in solvating power during the synthesis.[25] This is due to the fact that at higher temperature the reaction is accelerated and the uniform homogeneity occurs quickly due to the increase in solvating power. The pore size distribution for various hydrothermal temperatures was obtained (see Figure S3, Supporting Information). It is obvious that the cumulative pore size distribution was accumulated (narrow)[21] over a wide range, and the distribution of pore sizes increased uniformly upon increasing the hydrothermal temperatures. We observed a broad distribution of pore diameters of (20 to 50) Å for the mesoporous materials. Hence, increasing the temperature significantly increased the pore size distribution, surface area, and pore size. With respect to surface area, the porous materials followed the order ZC-16 > ZC-16-80 > ZC-16-60, and with respect to pore size, it was ZC-16 ≈ ZC-16−80 > ZC-16-60. These orders confirm that uniformly distributed porous materials possessing large surface areas could be obtained effectively at higher hydrothermal temperatures.

Effect of Calcination Temperature. We performed experiments at different calcination temperatures to study the effect of calcination. On the basis of the resulting pore size distributions, we found that the effect of calcination was insignificant. When we increased the calcination temperature from (500 to 600) °C, the surface area increased, but pore size decreased. When the calcination temperature was further increased to 700 °C, the surface area decreased, whereas the pore size remained approximately unchanged, suggesting that calcination at higher temperatures may lead to structural damage.

Effect of Filtration Method on Preparation. The effect of filtration was studied using both conventional filtration and dialysis membrane filtration. A comparison of both filtrations suggests that surface area of the porous materials was reduced when the synthesis method included dialysis membrane filtration, whereas the pore size was almost identical in both methods. One possible explanation for this behavior[26] is that a portion of the mesoporous materials was bound to or trapped in the membrane filter when we filtered a highly diluted solution. Therefore, to prevent erroneous results, it is recommended that the solutions be filtered at high concentration. So, it is concluded that dialysis membrane filtration is not advisible when attempting to prepare large surface area porous materials.

Effect of pH. To investigate the effect of pH, we performed syntheses at values of pH of 9 and 10. We suspected that high values of pH (pH 11 or 12) would not favor the formation of porous materials because the use of strong base to adjust the pH would surely inhibit the OH concentration and lead to structural disintegration of the alkyl silicates as indicated in eqs 1 and 2. Hence, the formation of reaction to obtain the porous materials at high pH is not easy. N_2 adsorption isotherms of the porous materials obtained at pH 9 and 10 were compared, and it can be noticed that hysteresis occurred (see Figure S2, Supporting Information) for ZC-16-P9 at values of P/P_0 ranging from 0.7 to 0.8 due to the proximity of the region of transition between irreversible and reversible adsorption behavior.[24,27] Comparison of the N_2 adsorption isotherms reveals that ZC-16 exhibited a sharp step in capillary condensation in the mesopores at a relative pressure of ca. 0.4, indicating its narrower pore size distribution relative to that of ZC-16-P9. In addition, the cumulative pore size distribution indicates that the accumulation of holes and the distribution of pores were larger in ZC-16 than in ZC-16-P9 (see Figure S4, Supporting Information). The mesopores had a broad distribution of pore diameters around (30 to 40) Å and (200 to 800) Å. Even though ZC-16 had a larger surface area and a greater pore size distribution, its pore size was significantly reduced relative to that of ZC-16-9 (see Table S1, Supporting Information).

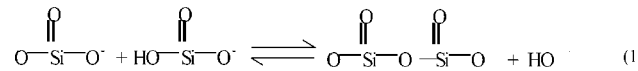

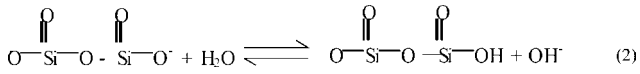

(2)

Adsorption of Heavy Metal Ions. Next we measured the adsorption ability of the as-synthesized mesoporous materials. In this experiment, adsorption of heavy metal ions such as Cu^{2+}, Ni^{2+}, and Pb^{2+} was carried out. For this purpose, various concentrations of (1 to 8) $mg \cdot L^{-1}$ of heavy metals were used in solutions and were mixed with 0.1 g of the adsorbent, and the adsorption behavior was studied after 24 h. Generally, Langmuir and Freundlich adsorption models are commonly used to study the adsorption phenomena.[28−30] To access the adsorption effect of adsorbents, the Langmuir linear adsorption model was used in this study. The adsorption of various metal ions (Pb^{2+} and Cu^{2+}) by different adsorbents is shown in Figure 4. The obtained adsorption data of metal ions and Langmuir parameters for all the adsorbents are given in Table 2. It can be seen from the results that in all cases the calculated R^2 value is found to be 0.9, indicating that the Langmuir isotherm model fitted the data well. The results suggest that the adsorption process involved a physical adsorption with the adsorption capacity depending upon the surface area and pore size of the adsorbents. This finding is supported by the fact that both physical and chemical adsorption processes are predominant as a function of the concentration range used.[31] At low concentration, essentially physical adsorption without excluding ion exchange becomes preponderant, and a remarkable deviation may occur at higher concentration. One possible explanation for physical adsorption occurring at lower concentration may be the release of weakly bonded ions into the solution, making it easy for metal ions to be removed through ion exchange.[32] Adsorption by each of the adsorbents increased upon increasing the initial concentration of the metal ions in solution. In all cases, when the initial concentration exceeded (3 to 4) $mg \cdot L^{-1}$, the adsorption capacity remained almost constant, presumably because at that initial concentration the active adsorption sites of the adsorbents were almost gradually filled by metal ions, and hence the adsorption activity was limited.[33] Thus, when the initial concentration of metal ions was increased further, no additional adsorption occurred because of the unavailability of adsorption sites suggesting that an optimal concentration of metal ions existed for effective adsorption. These experiments vividly reveal that the choice of preparation conditions altered not only the surface morphology of the adsorbents but also the extent of their adsorption of metal ions.

Comparison of Adsorption Capacity of Heavy Metal Ions. On the basis of the experimental results, it is observed that among the heavy metal ions tested the adsorption behavior[32] of Pb^{2+} was appreciably higher than that of the remaining metal ions with the selectivity sequence being $Pb^{2+} > Cu^{2+} > Ni^{2+}$. This could be attributed to the relatively larger size, larger ionic radius, and higher electronegativity of Pb.[34,35] Heavy metal ion uptake can occur through several different mechanisms involving ion-exchange and adsorption processes.[36] During the ion-exchange process, metal ions must move through both the pores and the channels of the lattice, and they must replace exchangeable cations. Diffusion is faster through the pores, but it is retarded when the pores are small. In this case, the metal ion uptake can mainly be attributed to ion-exchange reactions in the mesoporous medium. The heavy metal cations are present as hexaaqua complex ions in solution, with six surrounding water molecules, and they must pass through the pores in this form. Since the adsorption phenomenon depends on the charge density of cations, the diameter of the hydrate cations is very important as the charges of the metal cations are the same (2+).[37] Adsorption values show that these metal ions were readily and rapidly adsorbed in the order $Ni^{2+} < Cu^{2+} < Pb^{2+}$, which agrees with the Irving−Williams series.[38] Notably, however, the selectivity for Pb^{2+} was greater than that for Cu^{2+} and Ni^{2+}, suggesting that the size of the pores played a vital role in the adsorption process. The reported adsorbents possessed suitably large surface areas to accommodate the metal ions, and we expected that the sizes of the tested metal ions would also be relatively sufficient. Note that if the size of the metal ions is either too low or too high the adsorption will be poor. The observed order of adsorption was possibly related to the differences in ionic radii.[34,35,39] Because the ionic radius of Pb^{2+} (1.19 Å) is greater than those of Cu^{2+} (0.73 Å) and Ni^{2+} (0.69

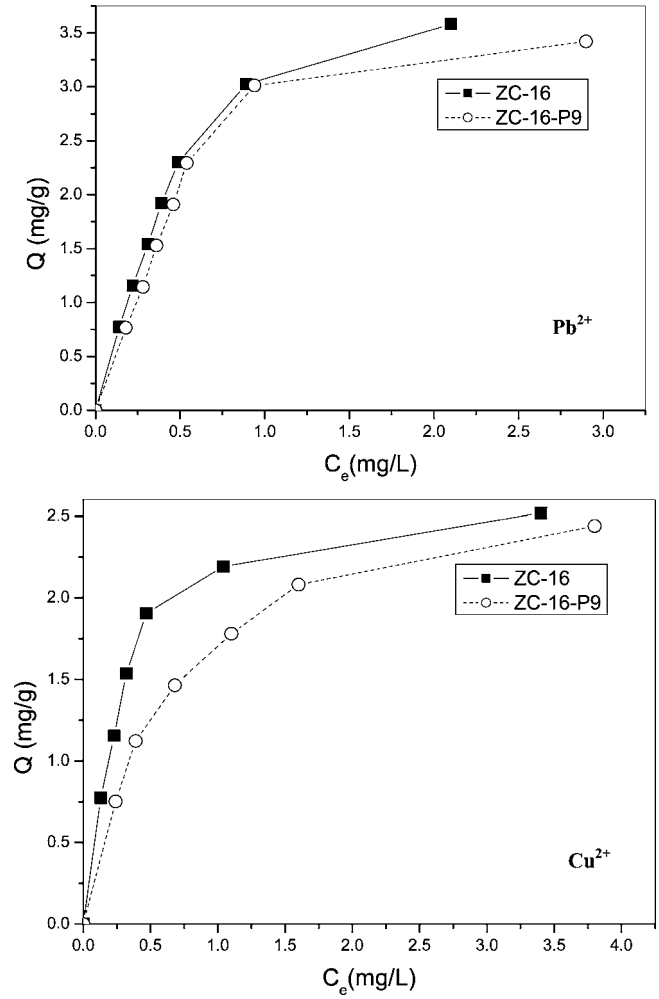

Figure 4. Adsorption of Pb^{2+} and Cu^{2+} ions by ZC-16-P9 and ZC-16.

Table 2. Adsorption of Heavy Metal Ions by Mesoporous Materials and Langmuir Isotherm Parameter

	adsorption of metal ions (q_m, $mg \cdot g^{-1}$)			R^2		
sample	Pb^{2+}	Cu^{2+}	Ni^{2+}	Pb^{2+}	Cu^{2+}	Ni^{2+}
ZC-16	6.61	3.46	2.25	0.9922	0.9907	0.9949
ZC-16-12H	5.34	2.21	1.24	0.9926	0.9908	0.9946
ZC-16-48H	5.45	2.31	1.89	0.9907	0.9978	0.9933
ZC-16-96H	5.62	2.51	2.13	0.9908	0.9944	0.9961
ZC-16-168H	5.57	2.11	1.91	0.0883	0.9914	0.9905
ZC-16-60	5.99	3.17	1.97	0.9946	0.9971	0.9975
ZC-16-80	6.12	3.32	2.06	0.9626	0.9484	0.9942
ZC-16-C	6.04	3.11	2.03	0.9891	0.9733	0.9975
ZC-16-P9	8.16	2.94	2.18	0.9738	0.9884	0.9949
PAC	-	2.01	-	-	0.9672	

Å), we would expect Pb^{2+} to be adsorbed to a greater degree. Our experimental observations suggest that the size and concentration of metal ions and the surface area and pore size of the adsorbents are all key factors that greatly affect the adsorption phenomenon. This study suggests that the adsorption capacity of the reported mesoporous materials is higher relative to that of commercially available PAC as shown in Table 2.

Conclusions

In this study, we examined the effects of various preparation conditions on the properties of mesoporous materials without functionalization. Among the obtained adsorbents, ZC-16 prepared at 100 °C for 24 h at pH 10 possessed both large surface areas and pore sizes revealing that the experimental conditions had a significant effect on the surface properties of mesoporous materials. SEM images of the adsorbents obtained under the various conditions clearly revealed their different surface areas and pore size distributions. The FT-IR spectra of the adsorbents provided strong evidence for the absence of the organic template. The mesoporous material synthesized at 100 °C for 24 h at pH 10 was the most effective adsorbent, and this synthesis was, therefore, considered to feature the optimal preparation conditions. Among the three metal ions tested, we found the mesoporus materials most effectively adsorbed Pb^{2+} ions. The degree of adsorption depended on surface area and pore size of the adsorbents and the size and concentration of metal ions in solution. The result of this study indicated that the adsorbents used in this present study were better than that of commercially available powdered activated carbon. This study suggests that a cost-effective and viable technology for the elimination of heavy metal ions from industrial wastewater can be developed using simple hydrothermal methods.

Supporting Information Available:

Supplementary table (Table S1) and figures (Figure S1 to S4). This material is available free of charge via the Internet at http://pubs.acs.org.

Literature Cited

(1) Chen, J. P.; Wang, X. Removing copper, zinc, and lead ion by granular activated carbon in pretreated fixed-bed columns. *Sep. Purif. Technol.* **2000**, *19*, 157–167.

(2) Gupta, V. K.; Ali, I. Utilisation of bagasse fly ash (a sugar industry waste) for the removal of copper and zinc from wastewater. *Sep. Purif. Technol.* **2000**, *18*, 131–140.

(3) Malkoc, E.; Nuhoglu, Y.; Dundar, M. Adsorption of chromium (VI) on pomace-An olive oil industry waste: batch and column studies. *J. Hazard. Mater.* **2008**, *138*, 142–151.

(4) Borba, C. E.; Silva, E. A. D.; Klen, M. R. F.; Kroumov, A. D.; Guirardello, R. Prediction of the copper (II) ions dynamic removal from a medium by using mathematical models with analytical solution. *J. Hazard. Mater.* **2008**, *152*, 366–372.

(5) Zhang, Y.; Banks, C. A comparison of the properties of polyurethane immobilised Sphagnum moss, seaweed, sunflower waste and maize for the biosorption of Cu, Pb, Zn and Ni in continuous flow packed columns. *Water Res.* **2006**, *40*, 788–798.

(6) Jusoha, A.; Lam, S. S.; Noraaini, A.; Noor, M. J. M. M. A simulation study of the removal efficiency of granular activated carbon on cadmium and lead. *Desalination* **2007**, *206*, 9–16.

(7) Feng, X.; Fryxell, G. E.; Wang, L.-Q.; Kim, A. Y.; Liu, J.; Kemner, K. M. Functionalized monolayers on ordered mesoporous supports. *Science* **1997**, *276*, 923–926.

(8) Brown, J.; Mercier, L.; Pinnavaia, T. J. Selective adsorption of Hg^{2+} by thiol-functionalized nanoporous silica. *Chem. Commun.* **1999**, 69–70.

(9) Liu, A. M.; Hidajat, K.; Kawi, S.; Zhao, D. Y. A new class of hybrid mesoporous materials with functionalized organic monolayers for selective adsorption of heavy metal ions. *Chem. Commun.* **2000**, 1145–1146.

(10) Bois, L.; Bonhomme, A.; Ribes, A.; Pais, B.; Raffin, G.; Tessier, F. Functionalized silica for heavy metal ions adsorption. *Colloids Surf. A: Physicochem. Eng. Aspects* **2003**, *221*, 221–230.

(11) Bibby, A.; Mercier, L. Mercury(II) ion adsorption behavior in thiol-functionalized mesoporous silica microspheres. *Chem. Mater.* **2002**, *14*, 1591–1597.

(12) Lee, B.; Kim, Y.; Lee, H.; Yi, J. Synthesis of functionalized porous silicas via templating method as heavy metal ion adsorbents: The introduction of surface hydrophilicity onto the surface of adsorbents. *Microporous Mesoporous Mater.* **2001**, *50*, 77–90.

(13) Yoshitake, H.; Yokoi, T.; Tatsumi, T. Adsorption of chromate and arsenate by amino-functionalized MCM-41 and SBA-1. *Chem. Mater.* **2002**, *14*, 4603–4610.

(14) Hossain, K. Z.; Mercier, L. Intraframework metal ion adsorption in ligand- functionalized mesoporous silica. *Adv. Mater.* **2002**, *14*, 1053–1056.

(15) Walcarius, A.; Etienne, M.; Bessiere, J. Rate of access to the binding sites in organically modified silicates. 1. Amorphous silica gels grafted with amine or thiol groups. *Chem. Mater.* **2002**, *14*, 2757–2766.

(16) Lee, H.; Yi, J. Removal of copper ions using functionalized mesoporous silica in aqueous solution. *Sep. Sci. Technol.* **2001**, *36*, 2433–2448.

(17) Merino, M. A. Á.; Ramon, V. L.; Castilla, C. M. J. A study of the static and dynamic adsorption of Zn(II) ions on carbon materials from aqueous solutions. *Colloid Interface Sci.* **2005**, *288*, 335–341.

(18) Goel, J.; Kadirvelu, K.; Rajagopal, C.; Garg, V. K. Removal of lead(II) by adsorption using treated granular activated carbon: batch and column studies. *J. Hazard. Mater.* **2005**, *B125*, 211–220.

(19) Amuda, S.; Giwa, A.; Bello, I. Removal of heavy metal from industrial wastewater using modified activated coconut shell carbon. *Biochem. Eng. J.* **2007**, *36*, 174–181.

(20) Nadeem, M.; Mahmood, A.; Shahid, S.; Shah, S.; Khalid, A.; McKay, G. Sorption of lead from aqueous solution by chemically modified carbon adsorbents. *J. Hazard. Mater.* **2006**, *138*, 604–613.

(21) Beck, J. S.; Vartuli, J. C.; Roth, W. J.; Leonowicz, M. E.; Kresge, C. T.; Schmitt, K. D.; Chu, C. T.-W.; Olson, D. H.; Sheppard, E. W.; McCullen, S. B.; Higgins, J. B.; Schlenker, J. L. A new family of mesoporous molecular sieves prepared with liquid crystal templates. *J. Am. Chem. Soc.* **1992**, *114*, 10834–10843.

(22) Selvam, P.; Bhatia, S. K.; Sonwane, C. G. Recent advances in processing and characterization of periodic mesoporous MCM-41 silicate molecular sieves. *Ind. Eng. Chem. Res.* **2001**, *40*, 3237–3261.

(23) Melis, K.; Vos, D. D.; Jacobs, P.; Verpoort, F. ROMP and RCM catalysed by $(R_3P)_2Cl_2Ru{=}CHPh$ immobilised on a mesoporous support. *J. Mol. Catal. A: Chem.* **2001**, *169*, 47–56.

(24) Gregg, S. J.; Sing, K. S. W. *Adsorption, Surface Area, and Porosity*, 2nd ed.; Academic Press: London, Inc., 1982.

(25) Darr, J. A.; Poliakoff, M. New directions in inorganic and metal-organic coordination chemistry in supercritical fluids. *Chem. Rev.* **1999**, *99*, 495–541.

(26) Baird, J. K.; Lambros, C. Effect of membrane filtration of antimalarial drug solutions on in vitro activity against *Plasmodium falciparum*. *Bull. World Health Org.* **1984**, *62*, 439–444.

(27) Kruk, M.; Jaroniec, M.; Sayari, A. Application of large pore MCM-41 molecular sieves to improve pore size analysis using nitrogen adsorption measurements. *Langmuir* **1997**, *13*, 6267–6273.

(28) Saygideger, S.; Gulnaz, O.; Istifli, E. S.; Yuxel, N. Adsorption of Cd(II), Cu(II) and Ni(II) ions by Lemna minor L effect of physico-chemical environment. *J. Hazard. Mater.* **2005**, *126*, 96–104.

(29) Ho, Y.-S. Selection of optimum isotherm. *Carbon* **2004**, *42*, 2115–2117.

(30) Vasanth Kumar, K.; Sivanesan, S. Sorption isotherm for safranin onto rice husk; comparison of linear and non-linear methods. *Dyes Pigm.* **2007**, *72*, 130–133.

(31) Prasad, M.; Saxena, S. Sorption mechanism of some divalent metal ions onto low-cost mineral adsorbent. *Ind. Eng. Chem. Res.* **2004**, *43*, 1512–1522.

(32) Prasad, M.; Saxena, S. Attenuation of divalent toxic metal ions using natural sericitic pyrophyllite. *J. Environ. Manage.* **2008**, *88*, 1273–1279.

(33) Say, R.; Denizli, A.; Arica, M. Y. Biosorption of cadmium (II), lead (II) and copper (II) with the filamentous fungus *Phanerochaete chrysosporium*. *Bioresour. Technol.* **2001**, *76*, 67–70.

(34) Boonamnuayvitaya, V.; Chaiya, C.; Tanthapanichakoon, W.; Jarudilokkul, S. Removal of heavy metals by adsorbent prepared from pyrolyzed coffee residues and clay. *Sep. Purif. Technol.* **2004**, *35*, 11–22.

(35) Mohan, S.; Gandhimathi, R. Removal of heavy metal ions from municipal solid waste leachate using coal fly ash as an adsorbent. *J. Hazard. Mater.* **2009**, *169*, 351–359.

(36) Baker, H. Characterization for the interaction of nickel(II) and copper(II) from aqueous solutions with natural silicate minerals. *Desalination* **2009**, *244*, 48–58.
(37) Baker, H.; Khalili, F. Comparative study of binding strengths and thermodynamic aspects of Cu(II) and Ni(II) with humic acid by Schubert's ion-exchange method. *Anal. Chim. Acta* **2003**, *497*, 235–248.
(38) Irving, H.; Williams, R. J. P. Order of stability of metal complexes. *Nature* **1948**, *162*, 746–747.
(39) Yavuz, Ö.; Altunkaynak, Y.; Güzel, F. Removal of copper, nickel, cobalt and manganese from aqueous solution by kaolinite. *Water Res.* **2003**, *37*, 948–952.

Received for review March 10, 2010. Accepted July 2, 2010. We thank the National Science Council (NSC), Taiwan, Republic of China (ROC), for financial support.

JE1002253